

Incomplete penetrance for isolated congenital asplenia in humans with mutations in translated and untranslated *RPSA* exons

Alexandre Bolze^{a,b}, Bertrand Boisson^{a,c,d,1}, Barbara Bosch^a, Alexander Antipenko^a, Matthieu Bouaziz^{c,d}, Paul Sackstein^a, Malik Chaker-Margot^e, Vincent Barlogis^f, Tracy Briggs^{g,h}, Elena Colinoⁱ, Aurora C. Elmore^j, Alain Fischer^{d,k,l,m,n}, Ferah Genel^o, Angela Hewlett^p, Maher Jedidi^q, Jadranka Keleci^r, Renate Krüger^s, Cheng-Lung Ku^t, Dinakantha Kumararatne^u, Alain Lefevre-Utile^v, Sam Loughlin^w, Nizar Mahlaoui^{d,k,l,n}, Susanne Markus^x, Juan-Miguel Garcia^y, Mathilde Nizon^z, Matias Oleastro^{aa}, Malgorzata Pac^{bb}, Capucine Picard^{d,k,cc}, Andrew J. Pollard^{dd}, Carlos Rodriguez-Gallego^{ee}, Caroline Thomas^{ff}, Horst Von Bernuth^{g,gg,hh}, Austen Worthⁱⁱ, Isabelle Meyts^{jj,kk}, Maurizio Risolino^{ll,mm,nn,oo,pp}, Licia Selleri^{ll,mm,nn,oo,pp}, Anne Puel^{a,c,d}, Sebastian Klinge^e, Laurent Abel^{a,c,d}, and Jean-Laurent Casanova^{a,c,d,l,qq,1}

^aSt. Giles Laboratory of Human Genetics of Infectious Diseases, Rockefeller Branch, The Rockefeller University, New York, NY 10065; ^bHelix, San Carlos, CA 94070; ^cLaboratory of Human Genetics of Infectious Diseases, Necker Branch, INSERM U1163, 75015 Paris, France; ^dImagine Institute, Paris Descartes University, 75015 Paris, France; ^eLaboratory of Protein and Nucleic Acid Chemistry, The Rockefeller University, New York, NY 10065; ^fPediatric Hematology, University Hospital of Marseille, 13005 Marseille, France; ^gManchester Centre for Genomic Medicine, Saint Mary's Hospital, Manchester University Hospitals NHS Foundation Trust Manchester Academic Health Sciences Centre, Manchester M13 9WL, United Kingdom; ^hDivision of Evolution and Genomic Sciences, School of Biological Sciences, The University of Manchester, Manchester M13 9NT, United Kingdom; ⁱDepartment of Pediatrics, Insular Maternity and Child University Hospital Center, 35016 Las Palmas de Gran Canaria, Spain; ^jNational Geographic Society, Washington, DC 20036; ^kINSERM U1163, 75015 Paris, France; ^lPediatric Hematology-Immunology and Rheumatology Unit, Necker Hospital for Sick Children, Assistance Publique – Hôpitaux de Paris (AP-HP), 75015 Paris, France; ^mCollege of France, 75231 Paris, France; ⁿFrench National Reference Center for Primary Immune Deficiencies (CEREDIH), Necker Hospital for Sick Children, AP-HP, 75015 Paris, France; ^oPediatric Immunology, Dr. Behcet Uz Children's Hospital, 35210 Izmir, Turkey; ^pDivision of Infectious Diseases, University of Nebraska Medical Center, Omaha, NE 68198; ^qDepartment of Legal Medicine, University Hospital Center Farhat Hached, Sousse, Tunisia; ^rDepartment of Pediatrics, University Hospital Center Zagreb, 10 000 Zagreb, Croatia; ^sDepartment of Pediatric Pneumology, Immunology and Intensive Care, Charité – Berlin University Hospital Center, 10117 Berlin, Germany; ^tGraduate Institute of Clinical Medical Sciences, College of Medicine, Chang Gung University, Taoyuan City 33302, Taiwan; ^uDepartment of Clinical Biochemistry and Immunology, Addenbrooke's Hospital, Cambridge University Foundation Hospitals NHS Trust, Cambridge CB2 0QQ, United Kingdom; ^vDepartment of Pediatrics, Infectious Diseases and Internal Medicine, Robert Debré Hospital, AP-HP, 75019 Paris, France; ^wMolecular Genetics, Great Ormond Street Hospital, London WC1N 3JH, United Kingdom; ^xMedical Genetics Dr. Staber & Kollegen Laboratory, 93051 Regensburg, Germany; ^yPediatric Immunology, Cruces University Hospital, 48903 Barakaldo-Vizcaya, Spain; ^zMedical Genetics Department, University Hospital of Nantes, 44000 Nantes, France; ^{aa}Department of Immunology and Rheumatology, Hospital de Pediatría J. P. Garrahan, 1249 Buenos Aires, Argentina; ^{bb}Department of Immunology, The Children's Memorial Health Institute, 04-730 Warsaw, Poland; ^{cc}Center for the Study of Primary Immunodeficiencies, Pediatric Immuno-Hematology Unit, Necker Children's Hospital, AP-HP, 75015 Paris, France; ^{dd}Oxford Vaccine Group, Department of Paediatrics, Oxford Children's Hospital, University of Oxford, Oxford OX4 2PG, United Kingdom; ^{ee}Department of Immunology, University Hospital of Gran Canaria Doctor Negrin, 35010 Las Palmas de Gran Canaria, Spain; ^{ff}Pediatric Oncology and Hematology, University Hospital of Nantes, 44000 Nantes, France; ^{gg}Department of Immunology, Labor Berlin GmbH, 13353 Berlin, Germany; ^{hh}Berlin-Brandenburg Center for Regenerative Therapies, 13353 Berlin, Germany; ⁱⁱPediatric Immunology, Great Ormond Street Hospital, London WC1N 3JH, United Kingdom; ^{jj}Department of Microbiology and Immunology, KU Leuven, BE-3000 Leuven, Belgium; ^{kk}Department of Pediatrics, KU Leuven, BE-3000 Leuven, Belgium; ^{ll}Institute for Human Genetics, University of California, San Francisco, CA 94143; ^{mm}Program in Craniofacial Biology, University of California, San Francisco, CA 94131; ⁿⁿEli and Edythe Broad Center of Regeneration Medicine & Stem Cell Research, University of California, San Francisco, CA 94131; ^{oo}Department of Orofacial Sciences, University of California, San Francisco, CA 94143; ^{pp}Department of Anatomy, University of California, San Francisco, CA 94143; and ^{qq}Howard Hughes Medical Institute, The Rockefeller University, New York, NY 10065

Contributed by Jean-Laurent Casanova, June 26, 2018 (sent for review March 30, 2018; reviewed by Daniel L. Kastner and Vijay G. Sankaran)

Isolated congenital asplenia (ICA) is the only known human developmental defect exclusively affecting a lymphoid organ. In 2013, we showed that private deleterious mutations in the protein-coding region of *RPSA*, encoding ribosomal protein SA, caused ICA by haploinsufficiency with complete penetrance. We reported seven heterozygous protein-coding mutations in 8 of the 23 kindreds studied, including 6 of the 8 multiplex kindreds. We have since enrolled 33 new kindreds, 5 of which are multiplex. We describe here 11 new heterozygous ICA-causing *RPSA* protein-coding mutations, and the first two mutations in the 5'-UTR of this gene, which disrupt mRNA splicing. Overall, 40 of the 73 ICA patients (55%) and 23 of the 56 kindreds (41%) carry mutations located in translated or untranslated exons of *RPSA*. Eleven of the 43 kindreds affected by sporadic disease (26%) carry *RPSA* mutations, whereas 12 of the 13 multiplex kindreds (92%) carry *RPSA* mutations. We also report that 6 of 18 (33%) protein-coding mutations and the two (100%) 5'-UTR mutations display incomplete penetrance. Three mutations were identified in two independent kindreds, due to a hotspot or a founder effect. Finally, *RPSA* ICA-causing mutations were demonstrated to be de novo in 7 of the 23 probands. Mutations in *RPSA* exons can affect the translated or untranslated regions and can underlie ICA with complete or incomplete penetrance.

Isolated congenital asplenia (ICA, MIM271400) is characterized by the absence of a spleen at birth in humans without other developmental defects. It renders otherwise healthy children susceptible to life-threatening invasive infections with encapsulated bacteria, typically *Streptococcus pneumoniae* but occasionally *Neisseria meningitidis* and *Haemophilus influenzae* b (1, 2). Asplenia can be detected by ultrasound (US) or computed tomography (CT)

Author contributions: A.B. designed research; A.B., B. Boisson, B. Bosch, A.A., M.B., P.S., and M.C.-M. performed research; V.B., T.B., E.C., A.C.E., A.F., F.G., A.H., M.J., J.K., R.K., C.-L.K., D.K., A.L.-U., S.L., N.M., S.M., J.-M.G., M.N., M.O., M.P., C.P., A.J.P., C.R.-G., C.T., H.V.B., A.W., and I.M. recruited the patients and provided clinical information; V.B., T.B., E.C., A.C.E., A.F., F.G., A.H., M.J., J.K., R.K., C.-L.K., D.K., A.L.-U., S.L., N.M., S.M., J.-M.G., M.N., M.O., M.P., C.P., A.J.P., C.R.-G., C.T., H.V.B., A.W., and I.M. contributed new reagents/analytic tools; A.B., B. Boisson, B. Bosch, M.B., M.C.-M., M.R., L.S., A.P., S.K., L.A., and J.-L.C. analyzed data; and A.B., B. Boisson, B. Bosch, and J.-L.C. wrote the paper.

Reviewers: D.L.K., National Institutes of Health; and V.G.S., Boston Children's Hospital.

Conflict of interest statement: A.B. works at Helix.

Published under the [PNAS license](#).

Data deposition: WES and RNA sequencing information reported in this paper has been deposited at the National Center for Biotechnology Information (BioProject nos. [SRP018839](#) and [PRJNA477701](#), respectively).

¹To whom correspondence may be addressed. Email: bebo283@rockefeller.edu or casanova@rockefeller.edu.

This article contains supporting information online at www.pnas.org/lookup/suppl/doi:10.1073/pnas.1805437115/-DCSupplemental.

Published online August 2, 2018.

isolated congenital asplenia | spleen | incomplete penetrance | ribosomopathy | *RPSA*

Significance

Isolated congenital asplenia (ICA) is characterized by the absence of a spleen at birth without any other developmental defect. ICA predisposes individuals to severe bacterial infections early in childhood. In 2013, we showed that very rare deleterious mutations in the protein-coding region of *RPSA*, which codes for a protein in the ribosome, caused ICA in 8 of 23 kindreds. We have since enrolled 33 more kindreds and identified 11 new ICA-causing *RPSA* protein-coding mutations, as well as the first two ICA-causing mutations in the 5'-UTR of this gene. A few individuals carrying one of the new *RPSA* mutations had a spleen, indicating that mutations in *RPSA* can cause ICA with incomplete penetrance.

scans of the abdomen. The associated defect of spleen phagocytic function is confirmed by the detection of Howell–Jolly bodies on a blood smear. ICA is the only known developmental defect of humans restricted exclusively to a lymphoid organ, as the DiGeorge (3) and Nude (4) syndromes, for example, involve both the thymus and other tissues. A retrospective study in France showed that this condition affects at least 0.51 per 1 million newborns per year (2). However, the incidence of ICA is probably higher, as individuals with ICA may not present their first severe infection until adulthood (5) and may be incidentally diagnosed with ICA in the absence of infection (6–9). Most cases of ICA are sporadic, but multiplex kindreds exist, and the main mode of inheritance of ICA seems to be autosomal dominant (AD).

In 2013, we tested the hypothesis of genetic homogeneity underlying ICA in at least some unrelated patients, by looking for rare nonsynonymous variants of the same gene in several patients from different kindreds. Using whole-exome sequencing (WES), we identified seven heterozygous mutations of *RPSA* in 19 patients from 8 kindreds, among 36 patients from 23 kindreds studied in total (5). This includes individuals from these kindreds for whom we collected DNA after the publication of our original study. The mutations were located in protein-coding regions and included one frameshift duplication (p.P199Sfs*25) and one nonsense (p.Q9*) and five missense (p.T54N, p.L58F, p.R180W, p.R180G, and p.R186C) mutations. Mutations of *RPSA* were more frequent in familial than in sporadic cases, being detected in six of the eight multiplex kindreds (75%) and 2 of the 15 kindreds with sporadic disease (13%). All mutations were private to the ICA cohort, three occurred de novo (p.T54N, p.L58F, and p.R180W), and one (p.R180G) was recurrent, due to a mutational hotspot rather than a founder effect. Complete penetrance was observed in all 8 kindreds, as all 19 individuals carrying a rare heterozygous nonsynonymous mutation of *RPSA* had ICA. It should be noted that we did not investigate whether synonymous or non-protein-coding mutations in *RPSA* exons could cause ICA in our previous paper. Moreover, exon 1 of *RPSA*, which encodes only the 5'-UTR of *RPSA*, and the part of exon 7 encoding the 3'-UTR were not covered by the exome capture kit used in our previous study.

Since our first description of *RPSA* mutations in 2013, we have enrolled 37 additional ICA patients from 33 new and independent kindreds. Nine of these 33 kindreds approached us spontaneously after reading about our research online. Our international ICA cohort now comprises 73 patients from 56 kindreds with diverse ancestries and living on four continents (*SI Appendix, Fig. S1*). Patients were included if they had asplenia or a severely hypoplastic spleen documented by US, CT scan, or autopsy (10) (*SI Appendix, Fig. S2 and Table S1*) and excluded if they had other developmental defects, such as an associated congenital heart malformation (a type of heterotaxy known as Ivemark or asplenia syndrome) [Online Mendelian Inheritance in Man (OMIM) no. 208530]. The congenital nature of asplenia is documented at birth

in rare cases, occasionally inferred from family history in multiplex kindreds, but is typically suspected in index cases after an episode of invasive infection (*SI Appendix, Table S1*). The protein-coding region of *RPSA* was analyzed by Sanger sequencing in the 37 newly recruited patients, and we searched for *RPSA* copy number variation (CNV) by multiplex ligation-dependent probe amplification (MLPA) in kindreds with no mutations in the protein-coding regions of *RPSA*. We also tested the hypothesis that noncoding mutations of *RPSA* can underlie ICA. Sanger sequencing was, therefore, performed on exon 1 and the flanking intronic regions (the word “exon” will hereafter refer to the exon as well as the intronic bases at the intron–exon or exon–intron junctions) and the non-protein-coding parts of exons 2 and 7, which encode the 5'- and 3'-UTR of *RPSA*.

Results

A Model for the Genetic Architecture of ICA Caused by *RPSA* Mutations.

The field of human genetics has benefited from the recent release of large databases reporting allele frequencies for variants observed in the exomes (123,000) and genomes (75,000) of about 200,000 individuals (11). These new tools can be used to rule variants out as the cause of a disease on the basis of their allele frequency in the general population. However, several parameters (prevalence, inheritance, penetrance, and genetic and allelic heterogeneity) must be taken into account before defining the highest allele frequency in these databases considered plausible for an ICA-causing variant. Based on an estimate of about one in a million children being admitted to the hospital for ICA (2), and the fact that about 40% of individuals with ICA were never admitted to the hospital during childhood (10 of the 25 patients that were not on prophylactic antibiotics during childhood, in our cohort) (*Fig. 1A and SI Appendix, Table S1*) (5), we estimate the global prevalence of ICA to be about 1 in 600,000. We found mutations in the protein-coding sequence of *RPSA* to display complete penetrance for ICA in our previous study, but AD disorders by haploinsufficiency generally display incomplete penetrance (12, 13). We therefore chose to apply a model of high penetrance but not complete to be conservative and selected 75% penetrance. As variants of *RPSA* were shown to be the genetic cause of ICA in 8 of 23 kindreds in our previous study, we estimated the *RPSA* gene to be responsible for about 30% of ICA cases (genetic heterogeneity of 0.3). We observed the same mutation twice in the eight ICA kindreds with *RPSA* mutations. We therefore hypothesized that a single mutation could explain up to 25% of the ICA kindreds (allelic heterogeneity of 0.25). Using these estimates, we were able to calculate a maximum plausible allele frequency for an ICA-causing variant in a monoallelic dominant model, as follows: $AF_{max_mono} = (1/600,000) \times 0.25 \times 0.3 \times (1/0.75) \times (1/2) = 8.33 \times 10^{-8}$ (14). Therefore, in our monoallelic model, the maximum tolerated allele count for an ICA-causing variant in the two combined and complete databases (~200,000 individuals) would be 0 (95% CI). The maximum tolerated allele count for an ICA-causing variant in these databases restricted to whole-genome sequencing (WGS) (75,000 individuals) would also be 0. The seven nonsynonymous mutations identified in our 2013 study (5) are absent from the gnomAD and Bravo databases (accessed in February 2018) and, therefore, meet these criteria.

Identification of Previously Unknown Protein-Coding Mutations in *RPSA*.

We therefore hypothesized that nonsynonymous variants of *RPSA* absent from gnomAD and Bravo would be present in about a third of the newly recruited kindreds (*SI Appendix, Fig. S1*). Sanger sequencing of the protein-coding region of *RPSA* was performed for the 33 newly recruited kindreds. We identified 11 heterozygous coding mutations, in 12 kindreds, none of which was previously reported in ICA patients. None of these mutations is present in any of the public databases, or in our in-house cohort of 4,500 exomes from patients with various

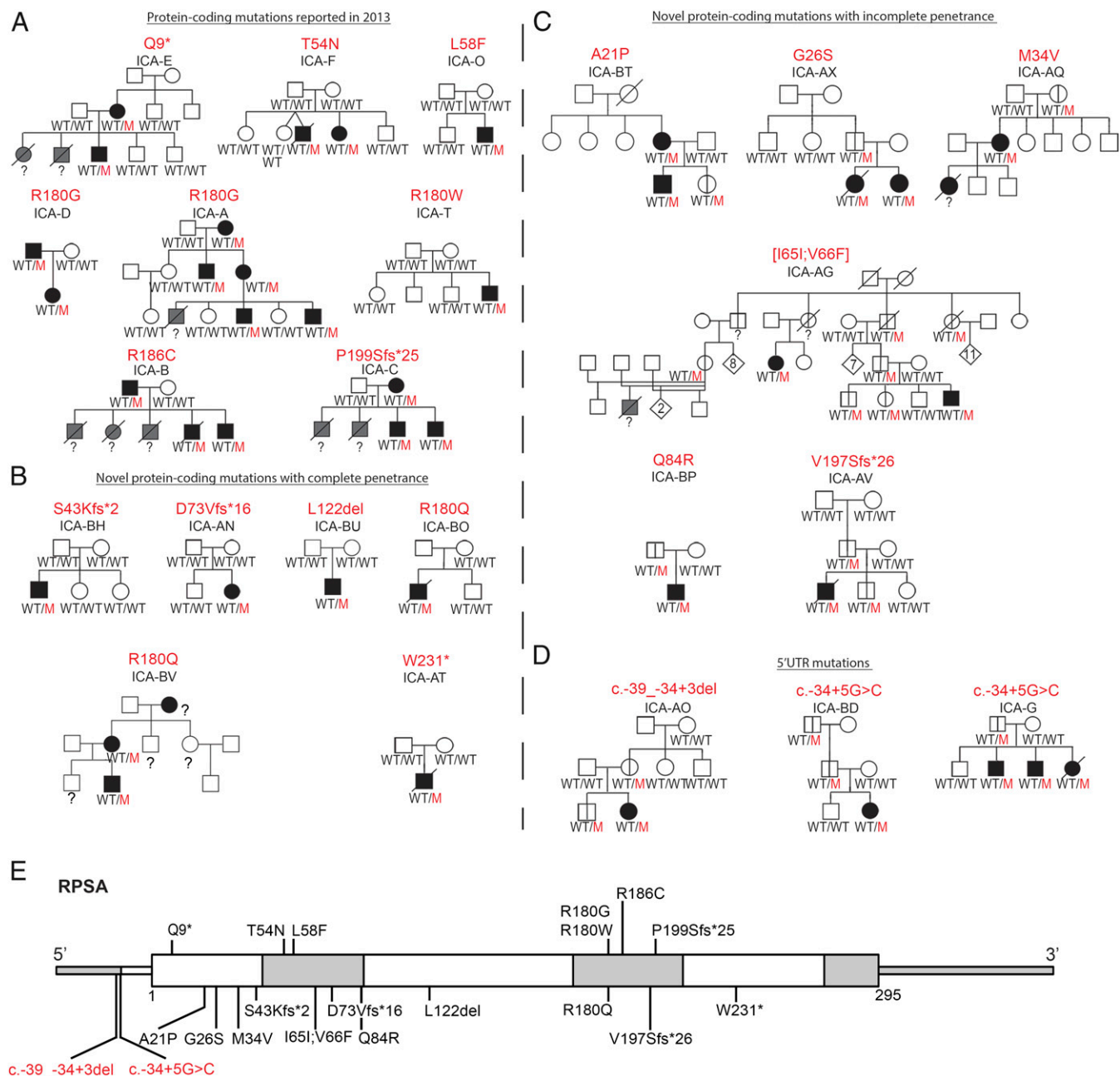


Fig. 1. Overview of the 23 ICA kindreds in our cohort who carry mutations in *RPSA*. (A) Eight kindreds were reported in our initial publication: All had nonsynonymous and fully penetrant mutations for ICA. (B and C) Twelve newly recruited kindreds had novel nonsynonymous mutations, displaying complete (B) or incomplete penetrance (C) for ICA. (D) Three ICA kindreds with mutations in the 5'-UTR of *RPSA*. (E) Schematic view of all of the ICA-causing mutations in *RPSA*. Mutations reported in our initial study are indicated above the gene schema. New mutations identified and reported in this study are indicated underneath the gene schema. Alternate white and gray color indicates the seven different exons from the canonical transcript of the gene (ENST00000301821).

infectious diseases (as of February 2018). The mutations can be grouped as (i) six missense mutations (p.A21P, p.G26S, p.M34V, p.[165I;V66F], p.Q84R, and p.R180Q), (ii) one in-frame deletion (p.L122del), (iii) three small frameshift insertions or deletions (p.S43Kfs*2, p.D73Vfs*16, and p.V197Sfs*26), and (iv) one nonsense mutation (p.W231*) (Fig. 1 B, C, and E). All known ICA patients in the new five multiplex families for whom DNA was available carried a missense mutation of *RPSA* (Fig. 1 B and C). No genomic DNA (gDNA) was available for one of the deceased ICA patients from family ICA-AQ, for another deceased individual who probably had ICA from family ICA-

AG, and for one ICA patient from family ICA-BV who was recently recruited to participate in the study. The mutations in kindreds ICA-AN, ICA-AT, ICA-BH, and ICA-BU were found to have occurred de novo, after microsatellite analysis (MSA) to validate parent-child relationships of the DNA samples we sequenced. The mutation observed in ICA-AV was found to have occurred de novo in the father of the index case (first-generation relative) (SI Appendix, Fig. S3). Mutation p.R180Q is recurring in two families, but we were not able to analyze the full haplotype around the mutation in family ICA-BO. Finally, we performed MLPA in the remaining kindreds, to detect CNVs

overlapping with the protein-coding region of *RPSA*. No CNVs were identified (*Methods*). The overall proportion of ICA kindreds carrying protein-coding mutations of *RPSA* (12 of the 33 new kindreds) is consistent with both our previous report (8 of the 23 previous kindreds) and our model for the genetic architecture of *RPSA* mutations underlying ICA.

The ICA Cohort Is Enriched in *RPSA* Protein-Coding Mutations. We then tested the hypothesis that these very rare nonsynonymous mutations of *RPSA* caused ICA, by comparing their frequency in the ICA cohort and the general population (15). The gnomAD and Bravo databases were considered the most suitable for such an *RPSA*-burden test as, together, they contain sequencing information for about 375,000 chromosomes, and the exome and genome sequences they contain provide good coverage of the protein-coding region of *RPSA*. We restricted our search to mutations of *RPSA* absent from the combined gnomAD and Bravo data, based on our previous estimates. Thus, for the calculation of *RPSA* burden, we considered only mutations that passed the quality filter and were present on no more than one chromosome in gnomAD and Bravo for our original comparison. We did not restrict our analysis to a specific population, as our cohort is diverse and the variants compared are extremely rare. We found that the newly recruited ICA kindreds, and the entire ICA cohort, were significantly enriched in very rare nonsynonymous variants, relative to the general population ($P = 2.44 \times 10^{-31}$ and $P = 9.95 \times 10^{-51}$, respectively) (Table 1). Restriction of the analysis to very rare missense variants and very rare in-frame indels revealed the newly recruited ICA kindreds, and the entire ICA cohort, to be significantly enriched in these variants ($P = 9.89 \times 10^{-21}$ and $P = 3.44 \times 10^{-35}$, respectively) (Table 1). Finally, we compared the nonsense, frameshift, and essential splicing mutations (in coding exons) in the ICA cohort with those present in the public databases, regardless of frequency. On the 375,000 chromosomes of gnomAD and Bravo, only two essential splice variants and three rare potentially damaging frameshift or nonsense variants (p.W176*, p.E235Vfs*60, and p.Q283*) were identified in the canonical ENST00000301821 transcript of *RPSA* (burden test, $P = 2.85 \times 10^{-19}$) (Table 1 and *SI Appendix, Fig. S4* and *Tables S2* and *S3*). The end of the *RPSA* sequence is less strongly conserved than the rest, so the frameshift of the last 60 aa and the p.Q283* mutation removing the last 12 aa may have little effect. Overall, these results confirm our original observation that very rare non-

synonymous mutations of *RPSA* cause ICA in about a third of the ICA kindreds.

Incomplete Penetrance of Some Novel Protein-Coding *RPSA* Mutations.

Unlike that of the original *RPSA* protein-coding mutations reported in eight ICA families (5), the penetrance for ICA of the mutations in 6 of the 12 new kindreds (50%) with new protein-coding mutations of *RPSA* was incomplete (Fig. 1C). Fifteen individuals carrying an ICA-causing mutation were found to have structurally and functionally normal spleens based on abdominal US or CT scans and/or the absence of Howell–Jolly bodies on blood smears. The distribution of these 15 asymptomatic carriers of *RPSA* mutation was as follows: p.A21P (1 of 3 carriers), p.G26S (1 of 3), p.M34V (1 of 2), p.[I65I; V66F] (9 of 11), p.Q84R (1 of 2), and p.V197Sfs*26 (2 of 3). We hypothesized that the nature of the *RPSA* mutation (e.g., its biochemical impact) contributes to the penetrance of ICA. We compared the Combined Annotation Dependent Depletion (CADD) scores of the mutations with their penetrance for ICA. CADD scores take into account information about evolutionary conservation, gene regulation, and transcription, to calculate the extent to which a nucleotide change is likely to be deleterious (*Methods*) (16). There was no significant difference between the mean CADD of incompletely penetrant compared with fully penetrant *RPSA* mutations (mean CADD 25.8 vs. 29.4, $P = 0.58$) (Fig. 2A and *SI Appendix, Fig. S4*). Similarly, other deleteriousness predictors did not show significant differences between the two sets of variants (*SI Appendix, Fig. S5*). We then mapped positions of the human mutations onto the human crystal structure of the small ribosomal subunit (Fig. 2B) (17). All five missense mutations with incomplete penetrance were found to be located outside of the hydrophobic core of *RPSA* lined with two α -helices (Fig. 2C and E). Amino acid 180, a mutational hotspot in ICA modified in 5 of 14 families with completely penetrant *RPSA* mutations, contacts the nearby α -helix and seems to stabilize the core (Fig. 2C and D). Moreover, all seven missense mutations with complete penetrance caused a change in the polarity or charge of the amino acid side-chain group, whereas p.M34V and p.V66F did not. These findings suggest that the incomplete penetrance of nonsynonymous mutations of *RPSA* may be due to the residual function of the protein, but further studies are required to understand the difference in penetrance of different *RPSA* mutations.

Table 1. Statistical analysis of nonsynonymous variants from ICA cohort vs. gnomAD and Bravo database

Category of variants	gnomAD + BRAVO total (WES + WGS)	Probands in original ICA kindreds 2013	Test*	Probands in new ICA kindreds 2017	Test†	Probands in entire ICA cohort	Test*
Total no. of chromosomes in group	375,000	46		66		112	
No. of chromosomes with a very rare nonsynonymous variant‡	86	8	2.97×10^{-21}	12	2.44×10^{-31}	20	9.95×10^{-51}
No. of chromosomes with a very rare missense variant or inframe indel	67	6	4.10×10^{-16}	8	9.89×10^{-21}	14	3.44×10^{-35}
No. of chromosomes with a nonsense, frameshift, or essential splice variant‡	5	2	3.09×10^{-07}	4	1.10×10^{-13}	6	2.85×10^{-19}

All of the variants used in the gene-burden tests are presented in *SI Appendix, Tables S2–S5*.

*Statistical significance threshold after correction with the stringent Bonferroni correction: 2.5×10^{-6} (note that in our original study, we only looked at 4,222 genes and therefore we originally used a P -value cutoff of 1.2×10^{-05}).

†Statistical significance threshold: 0.05.

‡Nonsynonymous variants were defined as nonsense, stop-loss, frameshift indels, inframe indels, missense, essential splice, and splice variants affecting exons 2–7. Splice variants affecting only exon 1 were not taken into account for the calculation concerning nonsynonymous variants, because exon 1 is noncoding, but they were analyzed in the UTR-burden test (Table 2).

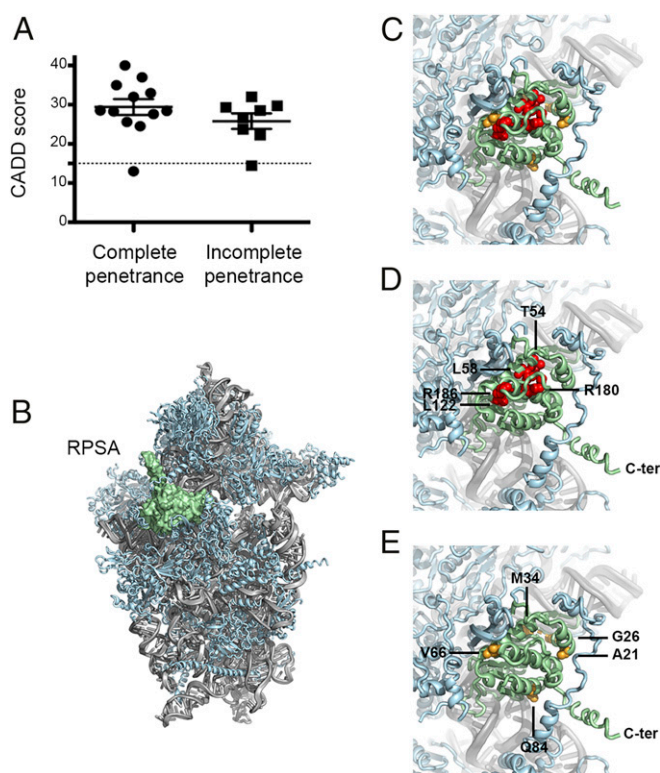


Fig. 2. Several mutations in *RPSA* display incomplete penetrance for ICA. (A) Comparative CADD score between *RPSA* coding-mutations leading to complete or incomplete penetrance. (B) Structure of the human small ribosomal subunit (PDB ID code 6EK0). The 18S ribosomal RNA is colored in gray, ribosomal proteins are colored in light blue, and *RPSA* is highlighted in green. (C–E) Detailed view of *RPSA* with colored spheres highlighting *RPSA* missense mutations leading to complete (red spheres) or incomplete (orange spheres) penetrance. Each amino acid found mutated in the ICA cohort is indicated based on human *RPSA*.

Identification of Mutations in the Non-Protein-Coding Region of *RPSA*.

We hypothesized that some cases of ICA may result from mutations in the noncoding region of *RPSA* exons. We searched for mutations in the 5'-UTR and 3'-UTR of *RPSA*, which are poorly covered by most WES kits. The 5'- and 3'-UTRs were subjected to Sanger sequencing in all 36 ICA kindreds of our cohort without very rare nonsynonymous mutations of *RPSA*. As for the candidate ICA-causing protein-coding mutations, we considered only mutations not present in gnomAD and Bravo. We identified two mutations predicted to affect the splicing of the 5'-UTR of *RPSA* that were private to our ICA cohort in three kindreds (Fig. 1D). There were no very rare or private 3'-UTR mutations. One mutation, c.-34+5G>C (canonical ENST00000301821 transcript), was recurrent. It was identified in both a multiplex kindred (ICA-G) and a patient with sporadic disease (ICA-BD). Another mutation, c.-39_-34+3del (ENST00000301821), was identified in a patient with sporadic disease (ICA-AO). These two mutations were absent from the 150,000 chromosomes sequenced by WGS in gnomAD and Bravo corresponding to the subset of samples with good coverage of exon 1 of *RPSA*. Both 5'-UTR splice mutations were heterozygous. As for some of the protein-coding mutations, penetrance was incomplete in ICA kindreds carrying a mutation in the 5'-UTR of *RPSA*: c.-34+5G>C (one in four of the individuals in ICA-G, and two of three in ICA-BD had a normal spleen) and c.-39_-34+3del (two of three). Overall, 3 of 36 ICA kindreds carried rare noncoding mutations in *RPSA* exons, whereas the overall proportion of ICA kindreds carrying a rare coding or noncoding mutation in *RPSA* exons was 23 of 56.

Enrichment of the ICA Cohort in *RPSA* Noncoding Mutations. We tested the hypothesis that these very rare noncoding mutations of *RPSA* cause ICA, by comparing their frequency in the ICA cohort and the general population. In total, 26 chromosomes carried a very rare *RPSA* 5'-UTR variant (one chromosome in gnomAD WGS and Bravo; *SI Appendix*, Tables S4 and S5). Fisher's exact tests indicated that very rare mutations in the 5'-UTR or 3'-UTR of *RPSA* were more frequent in the ICA cohort than in the general population ($P = 9.75 \times 10^{-06}$; Table 2). These results suggest that the very rare noncoding mutations identified in ICA patients may cause ICA. We also identified a 5'-UTR variant (c.-47C>T) in three unrelated Western European families that was absent from the gnomAD database but present in Bravo, with an allele frequency of 3.9×10^{-05} . This variant was not retained as potentially disease-causing in our study, due to its allele frequency, but it might have a modifying effect (*Discussion*). The two kindreds carrying the c.-34+5G>C mutation were both from the United Kingdom. This mutation is not present in the UK10K dataset (18) corresponding to high-quality WGS data for 3,781 samples. We investigated whether this very rare variant was recurrent due to a founder effect or a mutational hotspot. We defined the haplotypes encompassing this mutation in both kindreds. We identified an 850-kb region with a haplotype of 250 SNPs common to the two kindreds. The length of this common haplotype strongly suggests that the mutation was inherited through a founder effect in both kindreds. Using ESTIAGE (19), we estimated the most recent common ancestor (MRCA) to have occurred 163 generations ago (95% CI [52–743]). Assuming a generation time of 25 y, the MRCA was estimated to have lived 4,075 years ago (95% CI [1,300–18,575]). The ICA cohort is, thus, enriched in private 5'-UTR mutations, one of which is present in two distantly related families, with incomplete penetrance.

Functional Impact of the *RPSA* 5'-UTR Mutations. We investigated whether these 5'-UTR mutations were responsible for ICA, by studying their functional impact. The 5'-UTR of *RPSA* is not generally well conserved (*SI Appendix*, Fig. S5). However, the two mutations found in our ICA cohort are located at positions chr3:39,406,769 (hg38) and chr3:39,406,759–39,406,767, which are highly conserved between 100 vertebrate species (*SI Appendix*, Fig. S6) (18). This suggests that the 5'-UTR mutations identified in ICA patients may have a functional impact (*SI Appendix*, Fig. S4). We then used computational tools to construct hypotheses concerning the potential functional impact of these 5'-UTR mutations. The c.-34+5G>C mutation was predicted to impair splicing at the exon1/intron1 junction by disrupting the acceptor site [method: NNsplice9.0 (20)]. The c.-39_-34+3del mutation eliminates the exon1/intron1 splicing junction and would, therefore, also be predicted to impair the splicing of intron 1. NNsplice9.0 predicted that the next splicing site would be 70 bp further downstream. We also estimated the potential impact on splicing of the other 5'-UTR variants present in gnomAD or Bravo. Only two of these 52 variants were predicted to impair splicing, both disrupting the acceptor splicing site for the intron1/exon2 junction (*SI Appendix*, Table S6). We then experimentally tested the hypothesis that these ICA-associated 5'-UTR mutations impair splicing. RNA-sequencing (RNAseq) analysis confirmed the predictions made: both the c.-34+5G>C and c.-39_-34+3del mutations resulted in the retention of the same 70 bp (67 bp in the case of c.-39_-34+3del given that three nucleotides are deleted) (Fig. 3A). The two 5'-UTR mutations lead to a 50% WT:50% mutant allelic ratio (Fig. 3B). These 70 or 67 extra nucleotides contain two potential ATG codons (*SI Appendix*, Fig. S7). We also performed TOPO-TA cloning on cDNAs generated from peripheral blood mononuclear cells (PBMCs) from kindred ICA-G (c.-34+5G>C) (*SI Appendix*, Fig. S8). Again, we found that the c.-34+5G>C mutation prevented

Table 2. Statistical analysis of UTR variants from ICA cohort vs. gnomAD and Bravo database

Category of variants	Bravo + gnomAD (WGS)	ICA probands without nonsynonymous RPSA mutation	Test*	Probands in entire ICA cohort	Test*
Total no. of chromosomes in group	150,000	72		112	
All very rare 5'-UTR mutations	26	3	3.83×10^{-7}	3	1.45×10^{-6}
All very rare UTR mutations	51	3	2.58×10^{-6}	3	9.75×10^{-6}

*In this analysis, the 5'-UTR and 3'-UTR of RPSA are studied because RPSA is a candidate gene based on the protein-coding mutations in the same gene. This type of mutation was not studied in our initial cohort in 2013. Therefore, statistical significance threshold is set at 0.05. Statistical significance threshold after correction with the stringent Bonferroni correction is 2.5×10^{-6} .

correct splicing at the exon 1/intron 1 junction, creating an insertion of 70 bp at the end of exon 1. Both splice mutations of the 5'-UTR thus impair the structure but not the stability of the mRNA, contrasting with the completely penetrant p.D73Vfs*16 mutation, for which no RPSA transcript carrying the mutation (0/67) was identified by TOPO-TA cloning, likely due to nonsense-mediated decay. Overall, these results suggest that rare mutations with a significant impact on the 5'-UTR of RPSA probably cause ICA, with incomplete penetrance.

Discussion

We identified 11 protein-coding mutations and the first two noncoding mutations of RPSA responsible for ICA. Mutations in RPSA exons underlie ICA in 41% of index cases and kindreds (23 of 56 kindreds). This proportion differs significantly between

multiplex kindreds (such mutations were found in 12 of 13 multiplex kindreds, 92%) and kindreds affected by sporadic ICA (11 of 43 kindreds, 24%). Mutations in RPSA exons were found to cause ICA in about half the patients (40 of 73) from the 56 kindreds included in our international ICA cohort. None of the mutations identified were present in any variant database we looked at, which included more than 375,000 chromosomes. The burden of de novo RPSA mutations was high, with at least 7 of the 23 probands in kindreds with RPSA mutations carrying a de novo RPSA mutation. These results build on our previous report (5), as we have now identified mutations affecting both protein-coding and noncoding regions of the exons of RPSA. The genetic etiology of the ICA in kindreds without disease-causing mutations in the translated or untranslated regions of RPSA exons remains to be discovered. The relatively high frequency of RPSA mutations in this cohort suggests that other mutations may be present in regulatory regions outside of the exons of RPSA in some of these patients. A similar situation has been reported for blepharophimosis-ptosis-epicanthus inversus syndrome, for which causal mutations have been identified as much as 300 kb upstream from FOXL2 (21).

An analysis of the relatives of ICA patients with RPSA mutations led to the identification of the first eight RPSA mutations with incomplete penetrance. This raises the question of the underlying cause for this interindividual variability in phenotype. Mutations with incomplete penetrance are not predicted to have a lower functional impact, compared with fully penetrant mutations, based on CADD or 11 other scores. As RPSA mutations cause ICA by haploinsufficiency, incomplete penetrance may be the result of hypomorphic mutations causing a smaller decrease of functional RPSA levels in heterozygotes than observed with loss-of-function mutations. The presence or absence of a modifier variant in a gene other than RPSA, or of an additional variant of RPSA (in cis or trans), rare or common, may also modulate the impact of the mutation (22). For example, an RPSA variant in trans to the mutation, increasing the levels of WT RPSA, may protect an individual heterozygous for a null or hypomorphic RPSA mutation. The analysis of the phenotypic variability between individuals carrying mutations in RPSA will either require a comprehensive analysis of very large kindreds, such as the ICA-AG kindred, or a sufficient level of genetic and perhaps allelic homogeneity across kindreds. An example of a common variant explaining the phenotypic variation in multiple individuals carrying a rare pathogenic variant is the digenic inheritance of nonsyndromic midline craniosynostosis caused by rare SMAD6 mutations and common BMP2 variants (23).

The RPSA gene encodes ribosomal protein SA, a core component of the small subunit of the ribosome (24). There are 80 known human ribosomal proteins (25). AD ICA most likely results from haploinsufficiency, rather than negative dominance, because of the high proportion of truncating mutations and the strong purifying selection operating on the RPSA locus (5). Noncoding 5'-UTR ICA-causing mutations of RPSA provide

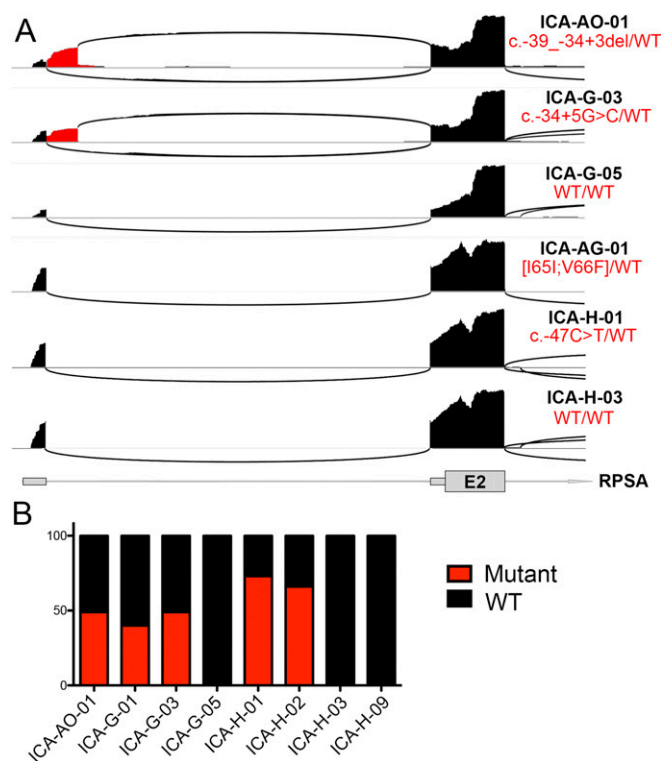


Fig. 3. Impact of the two 5'-UTR mutations on RPSA mRNA structure. The two 5'-UTR mutations identified in ICA patients impair the splicing of intron 1 and lead to an intron retention of 70 or 67 bp at the end exon 1. (A) Sashimi plots of RNAseq results for ICA-AO (c.-39_-34+3del), ICA-G (c.-34+5G>C), and ICA-H (variant c.-47C>T). In ICA-AO and ICA-G the mutations lead to a 67- or 70-bp intronic retention, respectively (red), whereas variant c.-47C>T does not impact mRNA structure (ICA-H). (B) Quantification of the allelic ratio. About half of the transcripts show the splicing defect in ICA-AO and ICA-G patients.

further support for a mode of action based on haploinsufficiency. The molecular and cellular mechanisms by which RPSA haploinsufficiency underlies ICA have remained elusive. Even more intriguingly, mutations of the genes encoding 15 other human ribosomal proteins cause Diamond-Blackfan anemia (DBA), including mutations of *RPS19*, the most common genetic etiology of DBA (26). DBA (OMIM no. 105650) is a ribosomopathy underlying a syndromic form of aplastic anemia. Patients typically present with normochromic macrocytic anemia together with growth retardation, and about 30–50% have congenital craniofacial, upper limb, heart, and/or urinary system malformations (27). None of the DBA patients reported in previous studies have asplenia, despite their wide range of developmental abnormalities. Conversely, none of the ICA patients apparently present any of the many hematological and developmental features of patients with DBA. The distinctive features of developmental tissues observed in the ribosomopathies underlying ICA and DBA, and emerging studies in other organisms suggest that the ribosome may influence the temporal and spatial control of gene expression during development. In an elegant study, lower amounts of ribosomes were shown to preferentially alter the translation of some transcripts, such as *GATA1*, thereby impairing erythroid lineage commitment and underlying DBA (28, 29).

Variable clinical expression, between patients and kindreds, of red-cell aplasia and congenital malformations has been widely reported for DBA (30, 31). The DBA-causing mutations of *RPS19* resulting in a severe clinical phenotype typically occur at a “mutation hot spot” in the core of the protein, which has a structure consisting of five α -helix bundles organized around a central amphipathic α -helix (32). In RPSA, arginine in position 180 is a hotspot for ICA-causing mutations and is also part of the core of the RPSA protein. We identified five completely penetrant mutations at the codon coding for R180. Incompletely penetrant mutations for both conditions map outside the core of the protein (Fig. 2 C–E). Moreover, the first exon of *RPS19*, like that of *RPSA*, is untranslated (5'-UTR) and the start codon is located at the start of exon 2. In addition to essential splice site mutations, one or two nucleotides downstream from the start codon of *RPS19* (33), rare 5'-UTR DBA-causing variants of *RPS19*, resulting in a longer 5'-UTR, have been shown to reduce RPS19 protein levels by 20%, modifying translational efficiency in a tissue-specific manner (34). The parallel between the *RPSA* mutations underlying ICA and the *RPS19* mutations underlying DBA is striking. In both cases, variants of both translated and

untranslated regions of the exons can be disease-causing, and both types of mutations can show incomplete penetrance.

Methods

Patients. The publication of our paper identifying RPSA variants as a genetic etiology of ICA led to additional referrals. Nine families, ICA-AG, ICA-AL, ICA-AM, ICA-AO, ICA-AQ, ICA-AR, ICA-BH, ICA-BP, and ICA-BO, approached us directly. Patients were recruited on the basis of three diagnostic criteria for ICA: (i) absence of a spleen on US or CT, or absence/presence of a splenic remnant on autopsy, (ii) presence of Howell-Jolly bodies on blood smear, and (iii) absence of heart abnormalities. After weighing up the pros and cons, we decided not to consider the members of ICA families with an accessory spleen as ICA patients. However, it seems plausible that a mutation leading to ICA may affect normal spleen development and results in the development of an accessory spleen. This would provide an argument for both individuals with no spleen and those with an accessory spleen being included in the “case” group for familial segregation analyses. However, accessory spleens are present in about 10% of the population, a frequency several orders of magnitude greater than that of total asplenia (35). As we have more than 50 kindreds enrolled in our cohort, we would expect there to be at least a few kindreds including individuals with an accessory spleen. We therefore decided not to consider these individuals as cases during familial segregation studies, and the absence of an *RPSA* mutation in these individuals would therefore not rule out the involvement of the mutation in ICA in other family members. In addition to studying the newly recruited families, we also updated the information for families reported in 2013. First, a newborn in family A was diagnosed with ICA. This baby carries the same missense mutation, p.R180G, as his relatives with ICA. Second, one patient, ICA-M-01, WT for *RPSA* has recently been diagnosed with Fanconi anemia, and we have identified compound heterozygous mutations of *FANCA*. Third, a sporadic boy (ICA-AH) has been found to carry a mutation in *ATRX*, which has been associated with asplenia as part of a broader syndrome in the past. He also suffers from mental retardation. We have retained these two kindreds in all of the calculations in this paper to ensure consistency with our first report. Finally, the reader may note several gaps in the “numbering” of the kindreds. For example, there is no kindred ICA-BA or ICA-BB, but there is an ICA-BC kindred. These gaps correspond to families or patients that have contacted us but that were not included in this study, for diverse reasons such as a lack of availability of DNA samples or of a signed informed consent form.

All experiments involving human subjects were conducted in accordance with local, national, and international regulations and were approved by the French ethics committee, ANSM (the French National Agency for the Safety of Medicines and Health Products) and the French Ministry of Research (protocol no. C10-16), and the Rockefeller University IRB (protocol no. JCA-0689). Informed consent was obtained from all participants included in this study.

Sanger Sequencing of the Seven Exons of RPSA. In addition to the primers used for sequencing exons 2–7, as described in our previous paper (5), we designed primers to sequence the 5'-UTR/exon 1 of *RPSA*. We also included

Table 3. Primers for amplification and sequencing of RPSA

Exon	Forward (F)/reverse (R)	Sequence (5' to 3')	Location of the primer	Primer_BLAST (no. of mismatches)
1	F	TGTA AACGACGCGCCAGTCTCTGGACAGGAATTATGCAC	5'-UTR isoform2	1 – chr 14
	R	CAGGAAACAGCTATGACCCGAGACAGATCCAGTCTGAC	Intron 1	3,286 bp (4+5)
2	F	TGTA AACGACGCGCCAGTCTCTGGACAGGAATTATGCAC	Intron 1	None
	R	CAGGAAACAGCTATGACCCAGACTAACCACGAGAATAGC	Intron 2	
3	F	TGTA AACGACGCGCCAGTCTCTGGACAGGAATTATGCAC	Intron 2	1 – chr 9
	R	CAGGAAACAGCTATGACCTGTCTCACAAATGCTGTAAGCT	Intron 3	1,077 bp (5+5)
4	F	TGTA AACGACGCGCCAGTGGAGTAGTAGTGATTAAGTTGGC	Intron 3	None
	R	CAGGAAACAGCTATGACCCCTACACTTGCGAGTTTCATCG	Intron 4	
5	F	TGTA AACGACGCGCCAGTGTATGTAAGAGCCAGGAAGTGC	Intron 4	1 – chr 12
	R	CAGGAAACAGCTATGACCTCTAGAAGCACAGTCCAAGTC	Intron 5	4,950 bp (5+5)
6	F	TGTA AACGACGCGCCAGTCTGTGGTTACATAAGCAAATTGG	Intron 5	1 – chr 7
	R	CAGGAAACAGCTATGACCCGAGTCTATCAGATGCTGTAGC	Intron 6	3,399 bp (4+5)
7	F	TGTA AACGACGCGCCAGTGTACAGCATCTGATAGACTGC	Intron 6	1 – chr 15
	R	CAGGAAACAGCTATGACCCGAGTACAACCTCATGTCCGAGAC	3'-UTR	4,737 bp (5+5)
M13F		TGTA AACGACGCGCCAGT		
M13R		CAGGAAACAGCTATGACC		

an M13 sequence in all primers (exons 1–7), to decrease the sequencing time. Primer-BLAST (<https://www.ncbi.nlm.nih.gov/tools/primer-blast/>) was used to check that the primers would not amplify another sequence from the human genome. Following the isolation of gDNA from EBV-B cells or PBMCs from patients and their relatives, each of the seven exons of *RPSA* was sequenced with these primers (listed in Table 3).

Allele Frequencies. The allele frequencies of *RPSA* variants present in the general population were retrieved from the exome and genome information in two public databases (last accessed February 2018). The gnomAD database contains 123,136 exome sequences and 15,496 whole-genome sequences from unrelated individuals sequenced as part of various disease-specific and population genetic studies. Information about *RPSA* can be obtained from the following URL: gnomad.broadinstitute.org/gene/ENSG00000168028, and the Bravo database lists genomic information for 62,784 possibly related individuals sequenced as part of NHLBI's TOPMed program. Information for *RPSA* can be obtained from <https://bravo.sph.umich.edu/freeze5/hg38/gene/ENSG00000168028>. We also interrogated the UK10K dataset (<https://www.uk10k.org/data.html>) to determine whether the variant identified in two kindreds from the UK was present in the general population of the United Kingdom. The UK10K dataset contains 3,781 low-depth whole-genome sequences and aims to characterize genetic variation exhaustively, down to a minor allele frequency of 0.1% in the British population. We also sequenced *RPSA* in 29 Japanese controls from the Centre de l'Étude de Polymorphisme Humain (CEPH) panel because of the Japanese origin of one side of the ICA-AG family. None of the 29 Japanese controls carried the p.[I65I; V66F] mutation.

Estimation of Allele Frequency for ICA. Maximum tolerated reference allele counts were calculated with the Frequency Filter available from <https://cardiodb.org/allelefrequencyapp/>. Based on the findings published in our first report, we predicted that ICA-*RPSA* would display monogenic inheritance, an incidence of about 1/600,000, an allelic heterozygosity of 0.25, a genetic heterozygosity of 0.3, and a penetrance of 0.75. Confidence was set at 0.95 and the reference population at 400,000 alleles.

Gene-Burden Tests. All of the data from public databases were downloaded on February 20, 2018. All variants with an impact on the canonical transcript ENST00000301821 were analyzed. Bravo and gnomAD differ in their representation of ENST00000301821, particularly at the end of exon 3. We used the gnomAD representation, which is identical to the Ensembl description. We also used the LiftOver tool (<https://genome.ucsc.edu/cgi-bin/hgLiftOver>) to facilitate comparisons between the two databases. We converted the GnomAD hg19 coordinates into hg38 coordinates and performed manual checks to ensure that this process did not introduce any errors.

Based on our model, we focused principally on variants present on only one chromosome in the public databases. However, about 3,000 whole-genome sequences are present in both gnomAD and Bravo. We therefore decided to retain a variant that was present on one chromosome in Bravo and one chromosome in gnomAD. However, we counted it as occurring on only one chromosome in this case (1 + 1 = 1). Other variants present on two chromosomes in either database were systematically filtered out (2 + 0 = 0).

Nonsynonymous variants were defined as nonsense, stop-loss, frameshift, missense, essential splice, and splice variants affecting exons 2–7. Splice variants affecting only exon 1 were not taken into account for the calculation concerning nonsynonymous variants, because exon 1 is noncoding, but they were analyzed in the UTR-burden test. Moreover, the whole-exome sequences of the gnomAD database do not cover this region. The c.*3_25delTGTTCTG-CATAGGCTCTTAAGC mutation was not taken into account for the loss-of-function variant-burden test, as the deletion results in the same 295 aa and termination codon. All of the variants used in the gene-burden tests are presented in supplementary tables (*SI Appendix, Tables S2–S5*).

We restricted our *RPSA*-burden tests to variants that passed the quality filter in gnomAD and Bravo, as most of the low-quality variants are false positives (36). Fisher exact tests were performed with R software:

```
input2.df = matrix(c(a,b,c,d), nrow = 2)
p_val = fisher.test(input2.df)$p.value.
```

MLPA for CNV Detection. We also searched for losses of one copy of *RPSA* as a cause of haploinsufficiency. We used the MLPA method, which has proved successful for the detection of CNVs in DBA (37). We designed probes mapping at least partly to the intronic region, because *RPSA* has several

pseudogenes. As controls, we used probes binding to chromosomes 18, X and Y. We also designed a probe binding upstream from exon 1 to cover a region including a 21-bp deletion SNP (rs199844419) that would impair the binding of the probe, as a proxy for a control for the loss of one copy of *RPSA*. Three individuals in our cohort are heterozygous carriers of this SNP. No kindred presented a loss of one copy of one *RPSA* probe except for the probe upstream of exon 1 in the individuals carrying the 21-bp deletion. We also searched the ExAC database (exac.broadinstitute.org/gene/ENSG00000168028) for the presence of CNVs in *RPSA*: None have been reported to date (last accessed January 2018). At the time of submission (March 2018), CNVs have not yet been included in the gnomAD or Bravo databases.

The MLPA protocol was performed using the reagent from MRC-Holland. Primers are listed in Table 4.

- The left and right probes (LPO and RPO) are mixed together to a final concentration of 200 nM each in 1× Tris-EDTA (10 mM Tris, pH 8.0 and 1 mM EDTA).
- All of the probes are then mixed and diluted using the volumes in Table 4 to prepare the Synthetic Basic Probemix.
- gDNA from individuals to be studied (100–150 ng) was resuspended in a total of 5 µL Tris-EDTA and denatured (98 °C, 5 min; 25 °C, 5 min).
- Synthetic Basic Probemix (1.5 µL) and MLPA buffer (1.5 µL) were added to the denatured gDNA and incubated at 95 °C for 1 min followed by 60 °C for 16–20 h for hybridization. Thirty-two microliters of ligase mix buffer was then added to the mix for a 15-min incubation at 54 °C, followed by an inactivation step (98 °C, 5 min). Amplification of the ligated products is performed by adding 10 µL of PCR mix (SALSA PCR) followed by PCR amplification for 35 cycles [95 °C, 30 s; (60 °C, 30 s, 72 °C, 1 min) ×35; 72 °C, 20 min; 15 °C].
- The separation of fragments by capillary electrophoresis were performed mixing 1 µL of undiluted PCR product to 9.0 µL formamide and 0.2 µL LIZ standard and then denatured at 85 °C for 2 min and held at 4 °C for a minimum of 5 min before analyzing using a ABI-3730 DNA analyzer.

***RPSA* Haplotypes Investigated by MSA (de Novo).** We determined whether the samples sequenced in kindreds in which *RPSA* mutations appeared de novo were of the expected origin (i.e., the sample labeled as the father indeed corresponded to DNA from the father, and that labeled as the mother indeed corresponded to the DNA of the mother; in other words, we checked that the parent–child relationships between the subjects were as indicated by the family and that there was no mixing up of the tubes at any point during the study). This was necessary to determine whether *RPSA* mutations truly occurred de novo in the ICA-AN, ICA-AT, ICA-AV, ICA-BH, and ICA-BU families. We thus analyzed microsatellites throughout the genome for the samples sequenced (proband, father and mother). MSA was performed with the Identifier Plus kit (Thermo Fisher Scientific) according to the manufacturer's protocol, optimized for use on an ABI Prism 3730 DNA analyzer (Applied Biosystems). PCR was first performed on a Veriti 96-well thermal cycler, with 10 µL AmpFISTR Identifier Plus Master Mix, 5 µL AmpFISTR Identifier Plus Primer Set, and 10 µL of a 0.1 ng/µL solution of DNA from the subject to be tested. The samples were then prepared for electrophoresis, using 1 µL of the PCR products or an allelic ladder and 9 µL of a 1:9 mixture of GeneScan™ 600 LIZ Size Standard and Hi-Di Formamide. Finally, data were analyzed with GeneMapper 4.0. The results are shown in *SI Appendix, Fig. S3*.

Haplotype Analysis for c.-34+5G>C. SNPs were genotyped with an Affymetrix 6.0 chip. After quality control (including a call rate of 100%), 909,622 SNPs were retained. Genotypes were phased with SHAPEIT v2 (38) software, with the 1000 Genomes Project samples as a reference panel. Familial information was used to improve the phasing and to identify the paternal haplotypes in which the mutation was located. We then determined the shared haplotype around the mutation and applied the likelihood-based ESTIAGE method (19) to estimate the age of the MRCA for the mutation. Recombination rates and haplotype frequencies MRCA were provided by the HapMap Project.

Prediction of the Impact of 5' UTR Mutations on mRNA Structure. We used the NNsplice 9.0 tool (www.fruitfly.org/seq_tools/splice.html) (20) to assess the potential impact on splicing of the rare variants at the exon1/intron1 splice junction identified in three kindreds with ICA. This tool has been shown to perform well for predicting the impact of variants leading to a splicing de-

Table 4. MLPA probe for CNV detection in RPSA

Name	Sequence*	Size fragment	Size	Probemix [†]	Volume used, μL
MLPA-RPSA-E1.2-LPO	GGGTTCCCTAAGGGTTGGAAAAAGCCAGTCCCAGCAGCGTTCTT	103	45	Ex 1.2	4
MLPA-RPSA-E1.2-RPO	p-CTCCGGCTCCGCCCTTCTTCCGCTCGACTTTCTTTCTAGATT-GGATCTTGCTGGCAC		58		
MLPA-RPSA-E2.2-LPO	GGGTTCCCTAAGGGTTGGAGACTGACTGACTGACTGACATGAAAA-GAAATAGTTGCTCTTATTTC	118	69	Ex 2.2	4
MLPA-RPSA-E2.2-RPO	p-GATTCGCCGTCGTAACCTAAAGGGAAATCTAGATTGGATCTTGC-TGGCAC		49		
MLPA-RPSA-E3-LPO	GGGTTCCCTAAGGGTTGGACAAGTGTACAAATCCTTCTGCCCTC-ACTTAG	107	51	Ex 3	3
MLPA-RPSA-E3-RPO	p-GCATCTATATCATAAATCTCAAGAGGACCTGGGTCTAGATTGG-ATCTTGCTGGCAC		56		
MLPA-RPSA-E4-LPO	GGGTTCCCTAAGGGTTGGAGAATATCGAGTACCCTAACTTTTAA-ATTCTCAAAG	114	56	Ex 4	4
MLPA-RPSA-E4-RPO	p-AGGGCTGTGCTGAAGTTGCTGCTGCCACTGGAGCTCTAGATT-GGATCTTGCTGGCAC		58		
MLPA-RPSA-E5-LPO	GGGTTCCCTAAGGGTTGGAGGTCATGCCTGATCTGTACTTCTACA-GAGATCCTGAAGAG	123	59	Ex 5	4
MLPA-RPSA-E5-RPO	p-GTAAGCTTCTCAAAGGCTTGTGGTTACATAAGCAAATTGGTC-TAGATTGGATCTTGCTGGCAC		64		
MLPA-RPSA-E7-LPO	GGGTTCCCTAAGGGTTGGATACATTGAGGACAGAGCTGATGGCTT-TTTTGGTATTCTCTTAAACAG	136	66	Ex 7	6
MLPA-RPSA-E7-RPO	p-AAGACTGGAGCGCTCAGCCTGCCACGGAAGACTGGTCTGCAGC-TCCCTCTAGATTGGATCTTGCTGGCAC		70		
MLPA-BCAP31-LPO	GGGTTCCCTAAGGGTTGGAAACAGGAGCCTGAAGGCTGACCT	91	41	BCAP31 (X)	4
MLPA-BCAP31-RPO	p-GCAGAAGCTAAAGGACGAGCTGGACTTCTAGATTGGATCT-TGCTGGCAC		49		
MLPA-SS18-LPO	GGGTTCCCTAAGGGTTGGACAGCAGCCACCTATGGGAATGATG	96	43	SS18	4
MLPA-SS18-RPO	p-GGTCAAGTTAACCAAGGCAATCATATGATGTCTAGATTGGA-TCTTGCTGGCAC		53		
MLPA-SRY-LPO	GGGTTCCCTAAGGGTTGGACAGCGAAGTGCAACTGGACAACAGGT-TGTA	100	49	SRY	4
MLPA-SRY-RPO	p-CAGGGATGACTGTACGAAAGCCACACTCTAGATTGGATCTT-GCTGGCAC		51		
MLPA-IFNG-LPO	GGGTTCCCTAAGGGTTGGATTGACTTCTCAGACTCTAAGGTCAAG-ATTAGCATTAAAAGGT	127	43	IFN-g (Chr. 12)	4
MLPA-IFNG-RPO	p-AATAGGAAATGTTTACAAAATAAAGTCAAAAAGTCTTAAAT-CTAGATTGGATCTTGCTGGCAC		42		
qs milliQ water					400

*Noted that all of the RPO primers have a 5'-phosphorylated nucleotides. Sequences in blue indicate universal primer sequence and sequence in green indicate specific RPSA sequence. qs, quantum stasis.

[†]Solution of 200 nM of each LPO and RPO probe.

fect (https://github.com/counsilresearch/posters/raw/gh-pages/2017/ASHG/Q506C_Tran_Intronic_Variants_V1_Final_PRINT.pdf).

RPSA Structure and Modeling of the Mutations. The structural data were obtained by mapping the positions of the human mutations onto the human crystal structure of the small ribosomal subunit [Protein Data Bank (PDB) ID code 6EK0] (17). All structural analyses and illustrations were made using PyMOL Molecular Graphics System, v.1.8 (Schrödinger).

RNAseq Preparation. Total cellular RNA was isolated from PBMCs with the RNeasy Mini kit (Qiagen). Multiplexed RNA libraries were prepared with the Truseq RNA sample prep kit (Illumina). In brief, poly(A)-containing mRNAs were captured with oligodT beads, fragmented, and reverse-transcribed, and the cDNA was ligated to Illumina adapters containing indexing barcodes. Libraries were quantified with KAPA Library Quant kits (KAPA Biosystems), and run on a HiSeq 2000 Sequencing System (Illumina) to produce 150-bp single-end reads. Reads were then mapped with STAR v2.5.3a. Sashimi plots were generated with IGV (Broad Institute), using a minimum threshold of 20 reads for a splice event to be taken into account. Accession ID: PRJNA477701.

TOPO-TA Cloning. RNA extracted from PBMCs was reverse-transcribed with the SuperScript III First-Strand synthesis system for RT-PCR kit (18080-051), following the manufacturer's protocol, with random hexamers. The TOPO

TA cloning kit for sequencing (450030; Invitrogen) was then used for subsequent cloning. The products were used to transduce Oneshot TOP 10 competent cells. Finally, we performed PCR on these colonies and sequenced them with the cRPSA-WT-11-R/cRPSA-WT-R6 primers (exons 1–4).

Prediction Software. We used 12 software tools for the prediction of the deleteriousness of missense or indel-frameshift mutations in ICA (CADD, Condel, Envision, FATHMM, Grantham, Mutation Assessor, MCAP, MPC, Polyphen2, Provean, Revel, and Sift). See *SI Appendix, Fig. S5* for data and references.

ACKNOWLEDGMENTS. We thank the patients and all of their families. Many of the new families in this study contacted us directly and devoted considerable effort and time to their participation in this study. We also thank Yelena Nemirovskaya, Dominick Papandrea, David Hum, Cécile Patisier, Benedetta Bigio, and Maya Chrabieh, who helped with all of the administrative questions and tasks required for this study. This work was supported in part by March of Dimes Grant 1-FY12-440, St. Giles Foundation, National Center for Research Resources and the National Center for Advancing Sciences of the National Institutes of Health Grant 8UL1 TR001866, the French National Agency for Research under the "Investissement d'avenir" program Grant ANR-10-IAHU-01, and the Integrative Biology of Emerging Infectious Diseases Laboratory of Excellence Grant ANR-10-LABX-62-IBED. A.B. was funded by a fellowship from the Jane Coffin Childs Memorial Fund for Medical Research from July 2014 to November 2015. B. Bosch was supported by a fellowship from the Boehringer Ingelheim Fonds.

1. Myerson RM, Koelle WA (1956) Congenital absence of the spleen in an adult; report of a case associated with recurrent Waterhouse-Friderichsen syndrome. *N Engl J Med* 254:1131–1132.
2. Mahlaoui N, et al. (2011) Isolated congenital asplenia: A French nationwide retrospective survey of 20 cases. *J Pediatr* 158:142–148, 148.e1.
3. Maggadottir SM, Sullivan KE (2013) The diverse clinical features of chromosome 22q11.2 deletion syndrome (DiGeorge syndrome). *J Allergy Clin Immunol Pract* 1: 589–594.
4. Palamaro L, et al. (2014) FOXN1 in organ development and human diseases. *Int Rev Immunol* 33:83–93.
5. Bolze A, et al. (2013) Ribosomal protein SA haploinsufficiency in humans with isolated congenital asplenia. *Science* 340:976–978.
6. Thiruppathy K, Privitera A, Jain K, Gupta S (2008) Congenital asplenia and group B streptococcus sepsis in the adult: Case report and review of the literature. *FEMS Immunol Med Microbiol* 53:437–439.
7. Gilbert B, et al. (2002) Familial isolated congenital asplenia: A rare, frequently hereditary dominant condition, often detected too late as a cause of overwhelming pneumococcal sepsis. Report of a new case and review of 31 others. *Eur J Pediatr* 161: 368–372.
8. Takahashi F, et al. (2008) Isolated congenital spleen agenesis: A rare cause of chronic thromboembolic pulmonary hypertension in an adult. *Respirology* 13:913–915.
9. Rose C, et al. (1993) [Congenital asplenia, a differential diagnosis of essential thrombocythemia]. *Presse Med* 22:1748.
10. Ferlicot S, Emile JF, Le Bris JL, Chéron G, Brousse N (1997) [Congenital asplenia. A childhood immune deficit often detected too late]. *Ann Pathol* 17:44–46.
11. Lek M, et al.; Exome Aggregation Consortium (2016) Analysis of protein-coding genetic variation in 60,706 humans. *Nature* 536:285–291.
12. Rieux-Laucat F, Casanova JL (2014) Immunology. Autoimmunity by haploinsufficiency. *Science* 345:1560–1561.
13. Boisson B, Quartier P, Casanova JL (2015) Immunological loss-of-function due to genetic gain-of-function in humans: Autosomal dominance of the third kind. *Curr Opin Immunol* 32:90–105.
14. Whiffin N, et al. (2017) Using high-resolution variant frequencies to empower clinical genome interpretation. *Genet Med* 19:1151–1158.
15. Lee S, Abecasis GR, Boehnke M, Lin X (2014) Rare-variant association analysis: Study designs and statistical tests. *Am J Hum Genet* 95:5–23.
16. Kircher M, et al. (2014) A general framework for estimating the relative pathogenicity of human genetic variants. *Nat Genet* 46:310–315.
17. Natchiar SK, Myasnikov AG, Kratzat H, Hazemann I, Klaholz BP (2017) Visualization of chemical modifications in the human 80S ribosome structure. *Nature* 551:472–477.
18. Pollard KS, Hubisz MJ, Rosenbloom KR, Siepel A (2010) Detection of nonneutral substitution rates on mammalian phylogenies. *Genome Res* 20:110–121.
19. Genin E, Tullio-Pelet A, Begeot F, Lyonnet S, Abel L (2004) Estimating the age of rare disease mutations: The example of Triple-A syndrome. *J Med Genet* 41:445–449.
20. Desmet FO, et al. (2009) Human splicing finder: An online bioinformatics tool to predict splicing signals. *Nucleic Acids Res* 37:e67.
21. Crisponi L, et al. (2004) FOXL2 inactivation by a translocation 171 kb away: Analysis of 500 kb of chromosome 3 for candidate long-range regulatory sequences. *Genomics* 83:757–764.
22. Castel SE, et al. (2017) Modified penetrance of coding variants by cis-regulatory variation shapes human traits. *bioRxiv*:10.1101/190397.
23. Timberlake AT, et al. (2016) Two locus inheritance of non-syndromic midline cranio-synostosis via rare *SMAD6* and common *BMP2* alleles. *eLife* 5:e20125.
24. Malygin AA, Babaylova ES, Loktev VB, Karpova GG (2011) A region in the C-terminal domain of ribosomal protein SA required for binding of SA to the human 40S ribosomal subunit. *Biochimie* 93:612–617.
25. Khatter H, Myasnikov AG, Natchiar SK, Klaholz BP (2015) Structure of the human 80S ribosome. *Nature* 520:640–645.
26. Mirabello L, et al. (2017) Novel and known ribosomal causes of Diamond-Blackfan anaemia identified through comprehensive genomic characterisation. *J Med Genet* 54:417–425.
27. Campagnoli MF, et al. (2008) RPS19 mutations in patients with Diamond-Blackfan anemia. *Hum Mutat* 29:911–920.
28. Ludwig LS, et al. (2014) Altered translation of GATA1 in Diamond-Blackfan anemia. *Nat Med* 20:748–753.
29. Khajuria RK, et al. (2018) Ribosome levels selectively regulate translation and lineage commitment in human hematopoiesis. *Cell* 173:90–103.e19.
30. Landowski M, et al. (2013) Novel deletion of RPL15 identified by array-comparative genomic hybridization in Diamond-Blackfan anemia. *Hum Genet* 132:1265–1274.
31. Narla A, et al. (2016) A novel pathogenic mutation in RPL11 identified in a patient diagnosed with diamond Blackfan anemia as a young adult. *Blood Cells Mol Dis* 61: 46–47.
32. Gregory LA, et al. (2007) Molecular basis of Diamond-Blackfan anemia: Structure and function analysis of RPS19. *Nucleic Acids Res* 35:5913–5921.
33. Boria I, et al. (2010) The ribosomal basis of Diamond-Blackfan anemia: Mutation and database update. *Hum Mutat* 31:1269–1279.
34. Badhai J, Schuster J, Gidlöf O, Dahl N (2011) 5'UTR variants of ribosomal protein S19 transcript determine translational efficiency: Implications for Diamond-Blackfan anemia and tissue variability. *PLoS One* 6:e17672.
35. Vikse J, et al. (2017) The prevalence and morphometry of an accessory spleen: A meta-analysis and systematic review of 22,487 patients. *Int J Surg* 45:18–28.
36. Durtschi J, Margraf RL, Coonrod EM, Mallempati KC, Voelkerding KV (2013) VarBin, a novel method for classifying true and false positive variants in NGS data. *BMC Bioinformatics* 14(Suppl 13):S2.
37. Quarello P, et al. (2008) Multiplex ligation-dependent probe amplification enhances molecular diagnosis of Diamond-Blackfan anemia due to RPS19 deficiency. *Haematologica* 93:1748–1750.
38. Delaneau O, Zagury JF (2012) Haplotype inference. *Methods Mol Biol* 888:177–196.